DOI: 10.1002/ejic.200801009

An Unsymmetrical Mixed-Valent Divanadium(IV/V) Complex

Anindita Sarkar[a] and Samudranil Pal*[a]

Keywords: Vanadium / Structure elucidation / Mixed-valent compounds / Chirality / Dinuclear complexes

In acetonitrile medium, reaction of bisacetylacetonatooxovanadium(IV) {[VO(acac)$_2$]} and acetylhydrazine ($CH_3CONHNH_2$) in a 2:1 molar ratio provides a novel, unsymmetrical, chiral, mixed-valent, triply bridged, dinuclear vanadium(IV/V) complex having the formula [(Hdmpz)OV(μ-acac)(μ-O)(μ-O_2CCH_3)VO(acac)] (Hdmpz = 3,5-dimethylpyrazole). The molecular structure of the complex was confirmed by X-ray crystallography. It crystallizes in the chiral space group $P2_12_12_1$ indicating a spontaneous resolution in the crystal. The complex is one-electron paramagnetic and redox active. It displays V^VV^{IV} to V^VV^V oxidation and V^VV^{IV} to $V^{IV}V^{IV}$ reduction responses. The crystal structure and EPR measurements revealed the trapped-valent character of the complex in the solid state as well as in the solution phase. Circular dichroism spectroscopic measurements with a powdered sample revealed that the bulk material is not racemic. In solution, the existence of both enantiomers of the complex is demonstrated by the Pfeiffer effect with the use of L- and D-arabinose as environment substances.

Introduction

The chemistry of oxovanadium species is an area of intense research activity due to its biological, pharmaceutical, and industrial significance.[1–12] Complexes of the mixed-valent $\{OV(\mu\text{-}O)VO\}^{3+}$ core are of particular interest for their molecular and electronic structures. Structurally characterized complexes containing the $\{OV(\mu\text{-}O)VO\}^{3+}$ core are very few.[13–24] In all these complexes, the metal ions are bridged by only the oxo group and they are symmetric with respect to the ligands bonded to them. Only in one case do the two ligands attached to the two metal centers differ in the substituents attached to them.[24] The reported structures have been scrutinized[19,24] for a correlation between the geometry of the $\{OV(\mu\text{-}O)VO\}^{3+}$ core and its electronic structure. It has been found that the *anti* linear configuration of the core facilitates a very effective overlap of the d_{xy} metal orbitals through the oxo bridge p_x orbital and, hence, a complete delocalization of the unpaired 3d electron over the two vanadium centers.[13,17,21] For an *anti* bent configuration, both localized and delocalized electronic structures are found. In these cases, the π basicity of the other coordinating atoms plays an important role in deciding the electronic structure.[19] Complexes with the *syn* bent $\{OV(\mu\text{-}O)VO\}^{3+}$ core are rare and they have localized electronic structures.[18,22,24] The lone example for a complex of $\{OV(\mu\text{-}O)VO\}^{3+}$ with a configuration in between *syn* and *anti* also has a localized electronic structure.[20] It is interesting to note that on the EPR timescale, except for very few cases,[19,21,24] valence-trapped species display delocalized electronic structures in the solution phase. In this work, we report the synthesis, characterization, and crystal structure of a complex containing the mixed-valent *syn*-$\{OV(\mu\text{-}O)VO\}^{3+}$ core, [(Hdmpz)OV(μ-acac)(μ-O)(μ-O_2CCH_3)VO(acac)] (Hdmpz = 3,5-dimethylpyrazole, acac = acetylacetonato). This complex is chiral and truly unsymmetrical with respect to the coordination environment around the two metal centers. Unlike the previously reported divanadium(IV/V) complexes, the present complex contains two additional bridges between the vanadium centers. The redox active complex is valence trapped in the solid state as well as in the solution phase. We also report the chirality of the bulk material and optical resolution of the complex in solution by using the Pfeiffer effect.[25]

Results and Discussion

Synthesis and Characterization

The dinuclear complex [(Hdmpz)OV(μ-acac)(μ-O)(μ-O_2CCH_3)VO(acac)] was synthesized by treating one mole equivalent of acetylhydrazine and two mole equivalents of bisacetylacetonatooxovanadium(IV) ([VO(acac)$_2$]) in acetonitrile under aerobic conditions. We repeated this reaction several times and each of these repetitions provided the complex in very similar (45–50%) yield. Thus, the synthetic procedure is reproducible. It is known that the reaction of acetylacetone with hydrazine produces 3,5-dimethylpyrazole (Hdmpz).[26] In all probability, the dissociation of a part of [VO(acac)$_2$] and the hydrolysis of acetylhydrazine provide acetylacetone and hydrazine, respectively, for the formation of the Hdmpz in the reaction mixture. The

[a] School of Chemistry, University of Hyderabad, Hyderabad 500 046, India
E-mail: spsc@uohyd.ernet.in

source of the bridging acetate group is the acetic acid produced in the hydrolysis of acetylhydrazine. The oxygen in air is responsible for the oxidation of a part of the vanadium(IV) to vanadium(V) during synthesis of the complex. If the reaction of $[VO(acac)_2]$ with acetylhydrazine is performed in dry acetonitrile under a nitrogen atmosphere the complex does not form. This observation corroborates to a certain extent the above-described pathway for the formation of the complex. However, despite several attempts we could not synthesize the complex by using $[VO(acac)_2]$, Hdmpz, and various salts of acetate as the starting materials. The elemental analysis data are consistent with the dinuclear molecular formula. The complex is electrically nonconducting in solution. The room-temperature (298 K) effective magnetic moment (1.70 μ_B) of the complex in the powder phase suggests the presence of an unpaired electron.

Description of the Molecular Structure

The complex crystallizes in the chiral space group $P2_12_12_1$. The molecular structure with the atom numbering scheme is shown in Figure 1. Bond parameters associated with the two metal centers are listed in Table 1. Both metal centers are in a distorted octahedral coordination geometry. The *cis* and *trans* bond angles are in the ranges 73.36(8)–104.16(12)° and 156.98(9)–177.5(1)°, respectively. The first metal center V1 is in the O_6 coordination sphere and the second metal center V2 is in the NO_5 coordination sphere. Although hexacoordinate, the metal center is significantly displaced towards the terminal oxo group in each case. The displacement of V1 from the square-plane formed by O1, O2, O5, and O8 (mean deviation 0.04 Å) is 0.297(1) Å and that of V2 from the square-plane formed by N1, O4, O6, and O8 (mean deviation 0.10 Å) is 0.286(1) Å. The metal centers are bridged by the oxo group, one acetylacetonate O atom, and the acetate. The bond lengths involving the bridging oxo group O8, the O atoms of the bridging acetate O5 and O6, and the terminal oxo groups O7 and O9 are significantly shorter at V1 than at V2 (Table 1). These bond lengths clearly indicate a trapped-valence situation, where V1 is in the +5 oxidation state and V2 is in the +4 oxidation state. However, the variations in the bond lengths involving the O atoms of the two acetylacetonate ligands are not straightforward with respect to the above oxidation state assignment as a result of the differences in their positions and the coordination modes (Figure 1, Table 1). The V1–O1 bond length [1.981(2) Å] *trans* to the acetate O atom is comparable to the V2–O4 bond length [1.988(2) Å]. Most likely the strong intramolecular N2–H···O1 hydrogen bond involving the Hdmpz N–H group (Figure 1) is the primary reason for the lengthening of the V1–O1 bond to a value that is comparable to the V2–O4 bond length. The N2–H, H···O1, and N2···O1 distances and the N2–H···O1 angle are 0.83(3), 2.12(4), and 2.934(4) Å and 165(4)°, respectively. For the bridging acetylacetonate O atom O3, the V–O bond length [2.357(2) Å] is significantly longer at V1 than that [2.196(2) Å] at V2. For both the metal centers, O3 is *trans* to the terminal oxo groups. Most likely a stronger *trans* influence by the short V=O bond at V1 compared to that by the long V=O bond at V2 on O3 causes this difference. Similarly the shorter V1–O8 bond [1.777(2) Å], relative to the V2–O8 bond [1.888(2) Å], causes the long V1–O2 [2.012(2) Å] and the short V2–O4 [1.988(2) Å] bonds, as both O2 and O4 are *trans* to the bridging oxo group O8. Thus, the V_2O_2 core is not symmetric with respect to the V–O bond lengths and it is folded along the O3···O8 line as a result of the additional acetate bridge. The fold angle is 20.4(1)°. The V–O–V bridge angle at the acetylacetonate O atom O3 is 87.54(7)°, whereas that at the oxo bridge O8 is 118.7(1)°. The O7–V1···V2–O9 torsion angle is 3.3(2)°. Thus, the $\{OV(\mu\text{-}O)VO\}^{3+}$ core has a near-perfect *syn* bent configuration with a V1···V2 distance of 3.1522(8) Å.

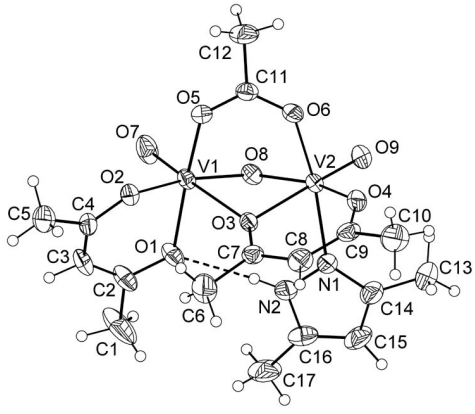

Figure 1. Molecular structure of [(Hdmpz)OV(μ-acac)(μ-O)(μ-O_2CCH_3)VO(acac)] with the atom labeling scheme. All non-hydrogen atoms are represented by their 30% probability thermal ellipsoids.

Table 1. Selected bond lengths and angles for $[V_2O_3(O_2CCH_3)(acac)_2(Hdmpz)]$.

Bond lengths [Å]			
V1–O1	1.981(2)	V2–N1	2.127(3)
V1–O2	2.012(2)	V2–O3	2.196(2)
V1–O3	2.357(2)	V2–O4	1.988(2)
V1–O5	1.988(2)	V2–O6	2.026(2)
V1–O7	1.577(2)	V2–O8	1.888(2)
V1–O8	1.777(2)	V2–O9	1.592(2)
Bond angles [°]			
O1–V1–O2	85.28(9)	N1–V2–O3	83.55(9)
O1–V1–O3	83.24(9)	N1–V2–O4	90.61(10)
O1–V1–O5	162.64(10)	N1–V2–O6	169.43(10)
O1–V1–O7	97.35(12)	N1–V2–O8	91.23(10)
O1–V1–O8	94.76(9)	N1–V2–O9	94.01(11)
O2–V1–O3	85.91(8)	O3–V2–O4	81.88(9)
O2–V1–O5	83.21(9)	O3–V2–O6	86.00(8)
O2–V1–O7	96.55(11)	O3–V2–O8	75.53(8)
O2–V1–O8	159.09(9)	O3–V2–O9	177.03(10)
O3–V1–O5	83.03(8)	O4–V2–O6	86.36(9)
O3–V1–O7	177.5(1)	O4–V2–O8	156.98(9)
O3–V1–O8	73.36(8)	O4–V2–O9	99.88(11)
O5–V1–O7	96.82(12)	O6–V2–O8	87.67(8)
O5–V1–O8	91.43(9)	O6–V2–O9	96.48(10)
O7–V1–O8	104.16(12)	O8–V2–O9	102.88(11)

Intermolecular Interactions and Self-Assembly

We investigated the self-assembly pattern of [(Hdmpz)-OV(μ-acac)(μ-O)(μ-O_2CCH_3)VO(acac)] in the crystal through intermolecular noncovalent interactions. Vanadium(IV/V)-bound oxo groups are known to participate as acceptors in intermolecular hydrogen-bonding interactions to provide various types of self-assembled networks.[27–31] Here, the bridging oxo atom O8 and one of the two terminal oxo atoms O9 are also involved in two intermolecular C–H···O interactions with the methyl groups belonging to the Hdmpz and acetylacetonate ligands, respectively. The C17···O8 and C5···O9 distances are 3.328(5) and 3.411(4) Å, respectively. The C17–H···O8 and C5–H···O9 angles are 146 and 147°, respectively. Both interactions generate right-handed helical structures (Figure 2). The helix formed due to the C5–H···O9 interaction propagates along the *b* axis and that formed by the C17–H···O8 interaction propagates along the *c* axis. These two essentially mutually perpendicular C–H···O interactions form a two-dimensional assembly of the complex molecules (Figure 3). There is no other significant noncovalent interaction between these layered structures.

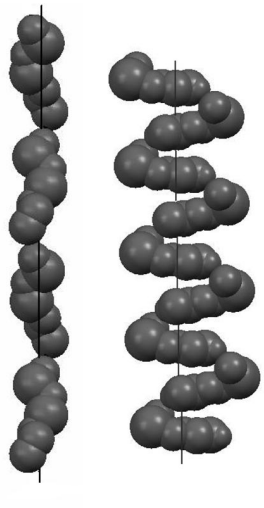

Figure 2. The right-handed helices along the (a) *b* and (b) *c* axis formed through intermolecular C5–H···O9 and C17–H···O8 interactions, respectively. For clarity, only the HC5C4O2V1O8V2O9 and HC17C16N2N1V2O8 atoms are shown in (a) and (b), respectively.

Electrochemical Properties

The electron transfer behavior of the complex in methanol solution was examined with the help of cyclic voltammetry. It displays two irreversible responses at the cathodic and anodic sides of the Ag/AgCl reference electrode (Figure 4). The former was observed at a platinum electrode, whereas the latter was observed at a glassy carbon electrode. The one-electron nature of each of these two responses is corroborated by comparing the peak current with known one-electron transfer processes under identical conditions.[31,32] The response at the cathodic side ($E_{1/2}$ = –0.21 V, ΔE_p = 270 mV) is assigned to the $V^{IV}V^{V} \rightarrow V^{IV}V^{IV}$ reduction and that ($E_{1/2}$ = 0.43 V, ΔE_p = 480 mV) at the anodic side is assigned to the $V^{IV}V^{V} \rightarrow V^{V}V^{V}$ oxidation.

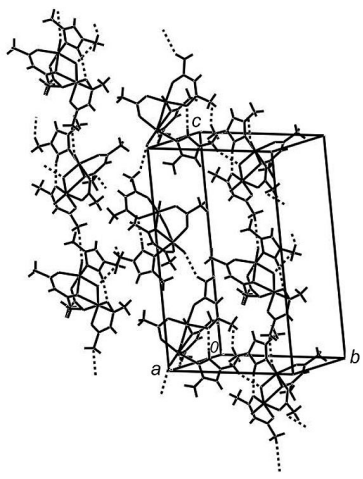

Figure 3. Two-dimensional network of [(Hdmpz)OV(μ-acac)(μ-O)(μ-O_2CCH_3)VO(acac)].

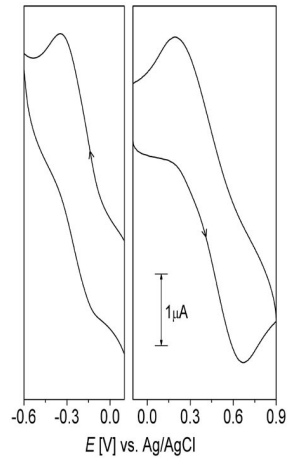

Figure 4. Cyclic voltammograms (scan rate 50 mVs^{-1}) of [(Hdmpz)-OV(μ-acac)(μ-O)(μ-O_2CCH_3)VO(acac)] in methanol (0.1 M TBAP) at 298 K.

Spectroscopic Properties

The complex displays three strong overlapping bands at 1582, 1557, and 1530 cm^{-1} in the infrared spectrum. The highest frequency band is assigned to the asymmetric stretching of the bridging acetate group, whereas the following two bands are assigned to the coupled C=C and C=O stretching modes of the acetylacetonate ligands.[33,34] The medium intensity band observed at 1433 cm^{-1} is attributed to the symmetric stretching mode of the bridging acetate group.[33,34] The N–H stretch of the Hdmpz appears as a broad band at 3270 cm^{-1}. A strong and a medium intensity band are observed at 986 and 965 cm^{-1}, respectively. These are assigned to the stretching frequencies of the two unsymmetrical terminal V=O bonds. Observation of such two

V=O stretching modes for trapped-valent complexes of $\{V_2O_3\}^{3+}$ core was previously reported.[19,24]

The electronic spectrum of the complex in methanol solution displays a low intensity broad shoulder centered at 535 nm. The origin of this broad shoulder is presumably a combination of more than one ligand-field transitions.[19–24] Following this weak absorption, a shoulder at 330 nm and a strong absorption at 275 nm are observed. These are assigned to the ligand-to-metal charge transfer and ligand-centered transitions. The complex does not display any low-energy absorption that can be attributed to intervalence transfer transition. The absence of an intervalence band indicates the trapped valent character of the complex in solution.

The EPR spectra of the complex in methanol at 298 and at 120 K are depicted in Figure 5. The room-temperature spectrum displays the clear eight line ^{51}V (I = 7/2) hyperfine structure. The g_{iso} and A_{iso} values are 1.984 and 97×10^{-4} cm^{-1}, respectively. Thus, as observed in the electronic spectrum, the observation of the eight line spectrum instead of the fifteen line spectrum further corroborates the rare valence localized situation in the solution phase for a complex with the $\{V_2O_3\}^{3+}$ core.[19,21,24] The frozen solution spectrum displays a typical well-resolved axial spectrum having $g_{\|}$ = 1.947 ($A_{\|}$ = 168×10^{-4} cm^{-1}) and $g_{\perp}$ = 1.986 ($A_{\perp}$ = 63×10^{-4} cm^{-1}).[20–22] It is well established that the parameters, particularly the hyperfine constants obtained from the EPR spectra of oxovanadium(IV) complexes, can be used to determine the type and number of the metal coordinating moieties with the help of the additivity relationship.[35] We calculated the $A_{\|}$ value for the present valence localized complex from the contributions to it by the equatorial coordinating atoms of the tetravalent metal center V2, namely the acetate O atom, the acetylacetonate O atom, the pyrazole N atom, and the bridging oxo group (Figure 1). As a result of the unavailability of the data for the pyrazole N atom and the bridging oxo group, we used the values for the imidazole N atom and the OH^- group, respectively.[35] The calculated $A_{\|}$ value (164.5×10^{-4} cm^{-1}) is very close to its value (168×10^{-4} cm^{-1}) determined from the frozen solution EPR spectrum of the complex.

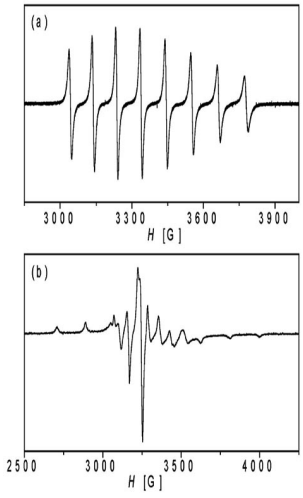

Figure 5. X-band EPR spectra of [(Hdmpz)OV(μ-acac)(μ-O)(μ-O_2CCH_3)VO(acac)] in methanol at (a) 298 and (b) 120 K.

Chirality of the Complex

The asymmetric molecules of [(Hdmpz)OV(μ-acac)(μ-O)(μ-O_2CCH_3)VO(acac)] crystallize in the chiral space group $P2_12_12_1$. Thus, there is a spontaneous resolution in the crystal of the complex. The chiral molecules self assemble into a two-dimensional layered structure composed of two mutually perpendicular right-handed helices formed through intermolecular C–H···O interactions (vide supra). To verify whether the bulk crystalline material is optically enriched or racemic we used circular dichroism (CD) spectroscopy. The spectrum was collected with a powdered sample taken in silicone oil. Interestingly the powdered crystalline material is CD active (Figure 6). Hence, there is not only spontaneous resolution in the single crystal but as a whole the crystalline bulk material is also enriched by a single enantiomeric form.

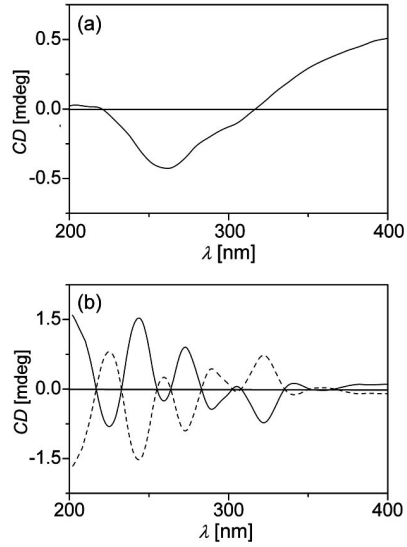

Figure 6. CD spectra of [(Hdmpz)OV(μ-acac)(μ-O)(μ-O_2CCH_3)-VO(acac)]: (a) powdered sample, (b) in solution with D-arabinose (—) and L-arabinose (- - -).

As expected in solution the complex is CD inactive as a result of racemization. However, with the help of the Pfeiffer effect,[25] optical resolution of the complex in solution has been achieved. In this effect, the racemate equilibrium is shifted in favor of one enantiomer in the presence of an enantiopure chiral compound as the environment substance. We used the L and D forms of arabinose (tetrahydropyran-2,3,4,5-tetraol) as the environmental substance. Both forms are insoluble in methanol but soluble in dimethyl sulfoxide. The electronic spectra of the complex in methanol and in dimethyl sulfoxide are essentially identical. Thus, the complex does not decompose in dimethyl sulfoxide. The dimethyl sulfoxide solution of the complex is CD inactive but in the presence of L- or D-arabinose it is CD active. The complex and arabinose were dissolved in di-

methyl sulfoxide in 1:2 molar ratio, the solution was left to stand for 12 h to attain the equilibrium, and then the CD spectra were recorded. These spectra (Figure 6) clearly show the presence of the two enantiomeric forms of the complex in solution. The O–H groups of arabinose can form hydrogen bonds with the oxo groups present in the complex.[36] Hence, the enantiomeric enrichment of the complex in solution most likely occurs due to the formation of its hydrogen-bonded aggregate with L- or D-arabinose. Formation of such aggregates is also indicated by a small but definite redshift in the electronic spectrum of the complex in the presence of L- or D-arabinose (Figure 7).

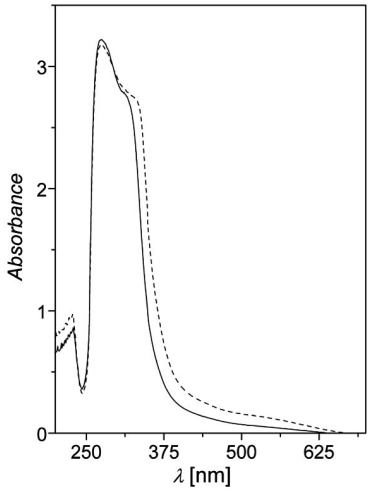

Figure 7. Electronic spectra of pure [(Hdmpz)OV(μ-acac)(μ-O)(μ-O_2CCH_3)VO(acac)] (—) and with D-arabinose (- - -) in dimethyl sulfoxide.

Conclusions

A novel unsymmetrical complex of the (μ-oxo)dioxovanadium(IV,V) core, $\{OV(\mu\text{-}O)VO\}^{3+}$, containing an acetate and an acetylacetonate as two additional bridges between the metal centers was synthesized and characterized. The complex [(Hdmpz)OV(μ-acac)(μ-O)(μ-O_2CCH_3)VO(acac)] crystallizes in the chiral space group $P2_12_12_1$, and the crystal structure revealed a valence-localized $\{OV(\mu\text{-}O)VO\}^{3+}$ core with a near perfect *syn* configuration and a very small V–O–V angle [118.7(1)°]. In the crystal lattice, self-assembly of the chiral complex molecules through two intermolecular C–H···O interactions leads to a two dimensional structure composed of two mutually perpendicular right-handed helices. This complex provides the rare example for a divanadium(IV,V) species having a valence-localized electronic structure in fluid solution at ambient temperature. It is very likely that the valence delocalization is prevented primarily by the very different coordination environment of the two metal centers. CD spectroscopic measurements with the powdered sample showed that the crystallization of the chiral complex from racemic solution results into optically enriched bulk material. The presence of both enantiomers of the complex in solution has been demonstrated by chiral discrimination activated by enantiopure arabinose as an environment substance. Currently, we are trying to synthesize analogous unsymmetrical complexes of $\{OV(\mu\text{-}O)VO\}^{3+}$ with different types of acid hydrazides.

Experimental Section

Materials: Bis(acetylacetonato)oxovanadium(IV)[37] and acetylhydrazine[38] were prepared by following reported procedures. All other chemicals and solvents used in this work were of analytical grade available commercially and were used as received.

Physical Measurements: A Thermo Finnigon Flash EA1112 series elemental analyzer was used for the elemental (C, H, N) analysis. Room-temperature (298 K) magnetic susceptibility was measured by using a Sherwood Scientific balance. A diamagnetic correction calculated from Pascal's constants[39] was used to obtain the molar paramagnetic susceptibility. A Digisun DI-909 conductivity meter was used to measure the solution electrical conductivity. Infrared spectra were recorded by using a KBr pellet with a Nicolet 5700 FT-IR spectrophotometer. Electronic spectra were recorded with the help of a Cary 100 Bio UV/Vis spectrophotometer. A Jeol JES-FA200 spectrometer was used to record the X-band EPR spectra. The circular dichroism spectra were recorded with a Jasco J810 spectropolarimeter. A CH-Instruments model 620A electrochemical analyzer was used for the cyclic voltammetric experiments with methanol solution of the complex containing tetrabutylammonium perchlorate (TBAP) as supporting electrolyte. The three electrode measurements were carried out at 298 K under a nitrogen atmosphere with a platinum disk or a glassy carbon working electrode, a platinum wire auxiliary electrode and an Ag/AgCl reference electrode. The potentials reported in this work are uncorrected for junction contributions.

[(Hdmpz)OV(μ-acac)(μ-O)(μ-O_2CCH_3)VO(acac)]: An acetonitrile solution (10 mL) of acetylhydrazine (74 mg, 1 mmol) was added to an acetonitrile solution (15 mL) of [$VO(acac)_2$] (530 mg, 2 mmol), and the mixture was heated in a water bath for 15 min. The resulting brown solution was allowed to evaporate in air at room temperature. The brown needle-shaped crystalline complex with a very little yellow powdery material separated in about 1–2 days, and it was collected by filtration. The solid thus obtained was treated with acetonitrile (10 mL) to dissolve the complex and then filtered to remove the insoluble powdery material. Slow evaporation of the clear filtrate at room temperature in air provided the pure dark brown crystalline complex. A single crystal for X-ray structure determination was collected from this material. Yield: 250 mg (50%). $V_2C_{17}H_{25}N_2O_9$ (503.27): calcd. C 40.57, H 5.01, N 5.57; found C 40.28, H 4.87, N 5.31. IR (KBr): $\tilde{\nu}$ = 3270 (m), 1582 (s), 1557 (s), 1530 (s), 1433 (m), 1362 (m), 1238 (s), 1144 (m), 986 (s), 965 (m), 801 (m), 673 (m), 586 (w), 465 (w), 422 (w) cm^{-1}. UV/Vis (CH_3OH): λ (ε, $M^{-1}cm^{-1}$) = 535 sh. (150), 330 sh. (2690), 275 (3140) nm.

X-ray Crystallography: The unit cell parameters and the intensity data were obtained with a Bruker-Nonius SMART APEX CCD single-crystal diffractometer equipped with a graphite monochromator and a Mo-K_a fine-focus sealed tube (λ = 0.71073 Å) operated at 2.0 kW. The detector was placed at a distance of 6.0 cm from the crystal. Data were collected at 298 K with a scan width of 0.3° in ω and an exposure time of 10 s/frame. The SMART software was used for data acquisition and the SAINT-Plus software was used for data extraction.[40] The absorption correction was performed with the help of the SADABS program.[41] The structure was solved in the space group $P2_12_12_1$ by direct method and refined

on F^2 by full-matrix least-squares procedures. The non-hydrogen atoms were refined by using anisotropic thermal parameters. The H atom of the NH group in Hdmpz was located in a difference Fourier map and refined with $U_{iso}(H) = 1.2U_{eq}(N)$. All other hydrogen atoms were included in the structure factor calculations at idealized positions by using a riding model. The SHELX-97 programs[42] available in the WinGX package[43] were used for structure solution and refinement. The ORTEX6a[44] and Platon[45] packages were used for molecular graphics. Selected crystal and refinement data are listed in Table 2. CCDC-705100 contains the supplementary crystallographic data for this paper. These data can be obtained free of charge from The Cambridge Crystallographic Data Centre via www.ccdc.cam.ac.uk/data_request/cif.

Table 2. Crystallographic data for $[V_2O_3(O_2CCH_3)(acac)_2(Hdmpz)]$.

Chemical formula	$V_2C_{17}H_{25}N_2O_9$
Formula weight	503.27
Crystal system	orthorhombic
Space group	$P2_12_12_1$
a [Å]	7.9322(19)
b [Å]	14.024(3)
c [Å]	20.541(5)
V [Å^3]	2285.0(9)
Z	4
$D_{calcd.}$ [g cm^{-3}]	1.463
μ [mm^{-1}]	0.865
Measured reflections	16244
Unique reflections	4483
Reflections $I \geq 2\sigma_I$	3925
R(int)	0.0381
Parameters refined	281
GOF on F^2	1.021
Flack parameter	0.02(2)
R_1, wR_2 ($I \geq 2\sigma_I$)	0.0372, 0.0832
R_1, wR_2 (all data)	0.0451, 0.0868
$\Delta\rho_{max}$, $\Delta\rho_{min}$ [e Å^{-3}]	0.283, –0.241

Acknowledgments

This work was supported by the Department of Science and Technology (DST), New Delhi (Grant No. SR/S1/IC-10/2007). A. S. thanks the Council of Scientific and Industrial Research, New Delhi for a research fellowship. X-ray structure was determined at the National Single Crystal Diffractometer Facility, School of Chemistry, University of Hyderabad (established by the DST). We thank the University Grants Commission, New Delhi for the facilities provided under the UPE and CAS programs.

[1] N. D. Chasteen (Ed.), *Vanadium in Biological Systems*, Kluwer, Dordrecht, **1990**.
[2] H. Sigel, A. Sigel (Eds.), *Metal Ions in Biological Systems: Vanadium and its Role in Life*, Marcel Dekker, New York, **1995**, vol. 31.
[3] C. G. Young, *Coord. Chem. Rev.* **1989**, *96*, 89.
[4] A. Butler, M. J. Clague, G. E. Meister, *Chem. Rev.* **1994**, *94*, 625.
[5] C. Slebodnick, B. J. Hamestra, V. L. Pecoraro, *Struct. Bonding (Berlin)* **1997**, *89*, 51.
[6] E. M. Page, *Coord. Chem. Rev.* **1998**, *172*, 111.
[7] D. Rehder, *Coord. Chem. Rev.* **1999**, *182*, 297.
[8] K. H. Thompson, J. H. McNeill, C. Orvig, *Chem. Rev.* **1999**, *99*, 2561.
[9] K. H. Thompson, C. Orvig, *Coord. Chem. Rev.* **2001**, *219–221*, 1033.
[10] A. G. T. Ligtenberg, R. Hage, B. L. Feringa, *Coord. Chem. Rev.* **2003**, *237*, 89.
[11] C. Bolm, *Coord. Chem. Rev.* **2003**, *237*, 245.
[12] T. Kiss, T. Jakusch, D. Hollender, Á. Dörnyei, É. A. Enyedy, J. C. Pessoa, H. Sakurai, A. Sanz-Medel, *Coord. Chem. Rev.* **2008**, *252*, 1153.
[13] M. Nishizawa, K. Hirotsu, S. Ooi, K. Saito, *J. Chem. Soc., Chem. Commun.* **1979**, 707.
[14] P. Blanc, C. Madic, J.-P. Launay, *Inorg. Chem.* **1982**, *21*, 2923.
[15] F. Babonneau, C. Sanchez, J. Livage, J.-P. Launay, M. Daoudi, Y. Jeannin, *Nouv. J. Chem.* **1982**, *6*, 353.
[16] A. Kojima, K. Okajaki, S. Ooi, K. Saito, *Inorg. Chem.* **1983**, *22*, 1168.
[17] J.-P. Launay, Y. Jeannin, M. Daoudi, *Inorg. Chem.* **1985**, *24*, 1052.
[18] J. C. Pessoa, J. A. L. Silva, A. L. Vieira, L. Vilas-Boas, P. O'Brien, P. Thornton, *J. Chem. Soc., Dalton Trans.* **1992**, 1745.
[19] D. Schultz, T. Weyhermüller, K. Weighardt, B. Nuber, *Inorg. Chim. Acta* **1995**, *40*, 217.
[20] S. Mondal, P. Ghosh, A. Chakravorty, *Inorg. Chem.* **1997**, *36*, 59.
[21] M. Mahroof-Tahir, A. D. Keramidas, R. B. Goldfarb, O. P. Anderson, M. M. Miller, D. C. Crans, *Inorg. Chem.* **1997**, *36*, 1657.
[22] S. K. Dutta, S. B. Kumar, S. Bhattacharyya, E. R. T. Tiekink, M. Chaudhury, *Inorg. Chem.* **1997**, *36*, 4954.
[23] R. A. Holwerda, B. R. Whittlesey, M. J. Nilges, *Inorg. Chem.* **1998**, *37*, 64.
[24] S. K. Dutta, S. Samanta, S. B. Kumar, O. H. Han, P. Burckel, A. A. Pinkerton, M. Chaudhury, *Inorg. Chem.* **1999**, *38*, 1982.
[25] P. Pfeiffer, K. Quehl, *Ber. Dtsch. Chem. Ges.* **1931**, *64*, 2667.
[26] R. H. Wiley, P. E. Hexner, *Org. Synth. Coll.* **1963**, *4*, 351.
[27] S. N. Pal, K. R. Radhika, S. Pal, *Z. Anorg. Allg. Chem.* **2001**, *627*, 1631.
[28] S. P. Anthony, L. Srikanth, T. P. Radhakrishnan, *Mol. Cryst. Liq. Cryst.* **2002**, *381*, 133.
[29] A. Sarkar, S. Pal, *Polyhedron* **2006**, *25*, 1689.
[30] A. Sarkar, S. Pal, *Polyhedron* **2007**, *26*, 1205.
[31] A. Sarkar, S. Pal, *Inorg. Chim. Acta* **2008**, *361*, 2296.
[32] S. G. Sreerama, S. Pal, *Inorg. Chem.* **2005**, *44*, 6299.
[33] H. J. Mok, J. A. Davis, S. Pal, S. K. Mandal, W. H. Armstrong, *Inorg. Chim. Acta* **1997**, *263*, 385.
[34] K. Nakamoto, *Infrared and Raman Spectra of Inorganic and Coordination Compounds*, Wiley, New York, **1986**, pp. 232–233 and 259–260.
[35] T. S. Smith II, R. LoBrutto, V. L. Pecoraro, *Coord. Chem. Rev.* **2002**, *228*, 1.
[36] V. Shivaiah, T. Arumuganathan, S. K. Das, *Inorg. Chem. Commun.* **2004**, *7*, 367.
[37] R. A. Rowe, M. M. Jones, *Inorg. Synth.* **1957**, *5*, 113.
[38] L. L. Koh, O. L. Kon, K. W. Loh, Y. C. Long, J. D. Ranford, A. L. C. Tan, Y. Y. Tjan, *J. Inorg. Biochem.* **1998**, *72*, 155.
[39] W. E. Hatfield, *Theory and Applications of Molecular Paramagnetism* (Eds.: E. A. Boudreaux, L. N. Mulay), Wiley, New York, **1976**, p. 491.
[40] *SMART 5.630 and SAINT-plus 6.45*, Bruker-Nonius Analytical X-ray Systems, Madison, WI, USA, **2003**.
[41] G. M. Sheldrick, *SADABS Program for Area Detector Absorption Correction*, University of Göttingen, Göttingen, Germany, **1997**.
[42] G. M. Sheldrick, *SHELX-97 Programs for Crystal Structure Analysis*, University of Göttingen, Göttingen, Germany, **1997**.
[43] L. J. Farrugia, *J. Appl. Crystallogr.* **1999**, *32*, 837.
[44] P. McArdle, *J. Appl. Crystallogr.* **1995**, *28*, 65.
[45] A. L. Spek, *PLATON A Multipurpose Crystallographic Tool*, Utrecht University, Utrecht, The Netherlands, **2002**.

Received: October 14, 2008
Published Online: January 14, 2009

